PROCEEDINGS OF SPIE

SPIEDigitalLibrary.org/conference-proceedings-of-spie

Whole-body visualization of nanoagent kinetics in mice with flash scanning volumetric optoacoustic tomography

Kalva, Sandeep Kumar, Ron, Avihai, Periyasamy, Vijitha, Reiss, Michael, Deán-Ben, Xosé Luís, et al.

Sandeep Kumar Kalva, Avihai Ron, Vijitha Periyasamy, Michael Reiss, Xosé Luís Deán-Ben, Daniel Razansky, "Whole-body visualization of nanoagent kinetics in mice with flash scanning volumetric optoacoustic tomography," Proc. SPIE 11642, Photons Plus Ultrasound: Imaging and Sensing 2021, 116420A (5 March 2021); doi: 10.1117/12.2577844



Event: SPIE BiOS, 2021, Online Only

Whole-body visualization of nanoagent kinetics in mice with flash scanning volumetric optoacoustic tomography

Sandeep Kumar Kalva^a, Avihai Ron^b, Vijitha Periyasamy^b, Michael Reiss^a, Xosé Luís Deán-Ben^a, and Daniel Razansky^{a,b,*}

^a Institute for Biomedical Engineering and Institute of Pharmacology and Toxicology, University of Zurich and ETH Zurich, Switzerland

^bInstitute for Biological and Medical Imaging, Technical University of Munich and Helmholtz Center Munich, Germany

*Corresponding author: Daniel Razansky, Institute of Biomedical Engineering, University of Zurich and ETH Zurich, HIT E42.1, Wolfgang-Pauli-Strasse 27, CH 8093 Zurich, Switzerland, Tel.: +41 44 633 34 29, daniel.razansky@uzh.ch

ABSTRACT

Visualizing whole-body dynamics across entire living organisms is crucial for understanding complex biology, disease progression as well as evaluating efficacy of new drugs and therapies. Existing small animal functional and molecular imaging modalities either suffer from low spatial and temporal resolution, limited penetration depth or poor contrast. In this work, we present flash scanning volumetric optoacoustic tomography (fSVOT) imaging system that enables the acquisition speeds required for visualizing fast kinetics and biodistribution of optical contrast agents across whole mice. fSVOT can render images of intricate vascular and organ anatomy with rich contrast by capitalizing on the large angular coverage of a spherical matrix array transducer rapidly scanned around the mouse. Volumetric (three-dimensional) images with 200 µm resolution can be acquired within 45 seconds, which corresponds to an imaging speed gain of an order of magnitude with respect to existing state-of-the-art modalities offering comparable resolution performance. We demonstrate volumetric tracking and quantification of gold nanorod kinetics and their differential uptake across the spleen, liver and kidneys. Overall, fSVOT offers unprecedented capabilities for multi-scale imaging of pharmacokinetics and bio-distribution of agents with high contrast, resolution and image acquisition speed.

Keywords: optoacoustic/photoacoustic imaging, whole-body imaging, contrast agents biodistribution, optoacoustic/photoacoustic tomography

1. INTRODUCTION

Several existing clinical imaging modalities such as computed tomography (CT), positron emission tomography (PET), single-photon emission computed tomography (SPECT), and magnetic resonance imaging (MRI) are being adapted for small animal imaging applications to study disease pathophysiology and monitor treatments¹. Other approaches based on superior functional and molecular optical contrast relying on fluorescence or optoacoustic (OA) excitation have further been developed². High spatiotemporal resolution is crucial in characterizing biodistribution, toxicity and metabolic clearance of drugs and contrast agents³. To this end, the evaluation of new therapies, accelerated drug discovery have been greatly facilitated by the pharmacokinetic studies assisted with targeted contrast agents in small animals⁴. To properly assess the dynamic biodistribution of the administered agents, the accelerated scanning time is essential. However, most of the small animal molecular imaging modalities need 20–30 min for a single total-body scan⁵, confining their applicability for efficient visualization of biological dynamics at the whole body level.

Recently, optoacoustic tomography (OAT) has been widely employed as a highly versatile molecular imaging technology for preclinical research⁶. It uniquely combines rich optical contrast with highly scalable ultrasound resolution to resolve various endogenous and exogenous substances with distinctive light absorption profiles⁷. For whole-body tomographic imaging of mice, OAT scanners based on different acquisition geometries and imaging speeds are increasingly exploited in various biological applications. For example, concave arrays of cylindrically focused

Photons Plus Ultrasound: Imaging and Sensing 2021, edited by Alexander A. Oraevsky Lihong V. Wang, Proc. of SPIE Vol. 11642, 116420A · © 2021 SPIE CCC code: 1605-7422/21/\$21 · doi: 10.1117/12.2577844

transducers provide cross-sectional (2D) views in real time, but lack the angular coverage required for accurate volumetric (3D) imaging ^{8, 9}. In order to achieve accurate reconstruction of arbitrarily oriented vascular structures, a large number of pressure signals should be acquired around the imaged object¹⁰. Recently, spiral volumetric optoacoustic tomography (SVOT) achieved unprecedented image quality at the whole-body level by exploiting the large angular coverage of a custom-made spherical array¹¹. This SVOT system has smartly further enabled scaling the effective temporal resolution to the desired field of view (FOV), for studying biological dynamics and biodistribution of agents. However, the high speed imaging was restricted to a small region or a single organ level¹². Generally, the state-of- the-art OAT system required at least 10–20 min to acquire high resolution total-body scans, which hampers the visualization of fast kinetics on a larger scale.

Herein, we demonstrate flash scanning volumetric optoacoustic tomography (fSVOT), that enables high-speed imaging of fast kinetics and biodistribution of optical contrast agents in whole mice¹³. This method effectively reduces high-resolution total body image acquisition times to sub-minute levels, an order of magnitude higher than existing state-of-the-art modalities, with unprecedented spatiotemporal resolution performance.

2. MATERIALS AND METHODS

2.1 fSVOT experimental set up

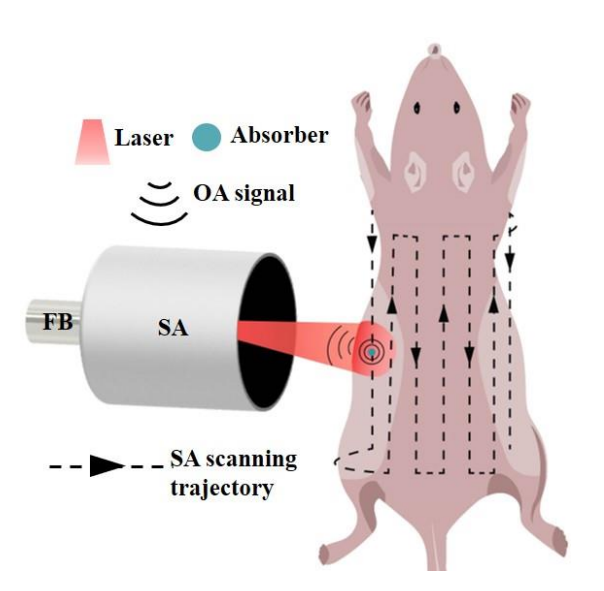


Figure 1. Schematic of the flash scanning volumetric optoacoustic tomography (fSVOT) scanner. OA: optoacoustic, FB: fiber bundle, SA: spherical array.

The schematic of the flash scanning volumetric optoacoustic tomography (fSVOT) scanner is shown in Fig. 1. A nanosecond (<10 ns) laser (SpitLight, Innolas Laser GmbH, Germany) operating at 1064 nm wavelength and at a pulse repetition frequency of 100 Hz was used as excitation light source. A spherical matrix transducer array (Imasonic SaS, Voray, France) mounted on motorized stages (IAI Inc., Japan) that are continuously rotated and vertically translated around the animal was used for detecting the generated OA signals. The spherical array consists of 256 elements (element area of 9 mm²) arranged on a hemispherical surface with a radius of 4 cm and 90° angular coverage¹⁴. The elements have central frequency of 4 MHz and -6 dB bandwidth of \approx 100%, resulting in nearly isotropic imaging resolution in the 150 μ m range¹¹. Light was guided via a custom-made fiber bundle through a central aperture of the array, thus creating a Gaussian illumination profile with a size of \approx 10 mm at the FWHM. The per-pulse energy at the fiber output was kept below 15 mJ. The spherical array was programmed to scan around the mice to complete a full 360° rotation in 18° steps. The recorded time-resolved OA signals were digitized at 40 MHz using a custom-made data acquisition system (DAQ; Falkenstein Mikrosysteme GmbH, Germany). The precise vertical position of the array was sampled by a sensitive (16 μ m resolution, sampling cycle-up to 3 μ s) laser displacement sensor (Keyence GmbH,

Germany). The Q-switch output of the laser simultaneously triggered the DAQ and displacement sensor. The data recorded by all the 256 channels were transmitted to a personal computer via 1 Gb Ethernet connection for further processing. Data acquisition and motor positioning were computer controlled using MATLAB (Mathworks, MA, USA).

2.2 Animal experiments: whole-body and biodistribution imaging

All animal *in vivo* experiments were performed on athymic nude-Foxn1 mice in full compliance with the Swiss Federal Act on Animal Protection and with approval by the Cantonal Veterinary Office Zurich (ZH 161/18). The mice were placed in a custom-made holder, which was used to maintain the mice in a stationary position along the center of rotational scanning. The fore and hind paws were attached to the holder and immersed inside the water tank with their head remaining outside the water. The temperature of the water tank was maintained at 34 °C with a feedback-controlled heating stick. A breathing mask with a mouth clamp was used to fix the head in an upright position and supply isoflurane anesthesia (4% v/v for induction and 1.5% v/v during the experiments Abott, Cham, Switzerland) in an oxygen/air mixture (100/400 mL/min) during the data acquisition. To prevent dehydration of eyes during scanning and to protect them from laser light, a vet ointment (Bepanthen, Bayer AG, Leverkusen, Germany) was applied on the eyes. While the animals were positioned inside the imaging setup, injections of 150 μ L gold nanorods (10 × 67 nm, surface plasmon resonance (SPR) wavelength = 1064 nm, 2.5 mg mL-1 phosphate buffer solution (PBS), Nanopartz Inc., USA) as well as 150 μ L of clean PBS for control experiments were done intravenously via a tail vein catheter (n = 3 mice).

2.3 Image reconstruction and analysis

The time-resolved signals from the 256 detection elements of the array were band-pass filtered between 0.1 and 6 MHz and deconvolved with the impulse response of the array elements. The filtered signals were used to reconstruct volumetric images covering $\approx 1~\rm cm^3$ FOV for each laser pulse using GPU implementation of a 3D back-projection algorithm¹⁵. A designated reconstruction approach of rapid spatial compounding of the volumes acquired in the overfly mode based on accurately synchronized laser distance sensors readings was employed. This was done by mapping the transducer elements' coordinates onto volumetric image grid (100 μ m/pixel) using known positions of the stages recovered from the displacement sensor's readings. 3D visualization of the OA images was achieved using Amira (Visual Sciences Group). A volumetric mask of each organ was manually delineated to quantify the changes in biodistribution of contrast agents across different organs. Next, the OA signal amplitude within each organ was quantified. Finally, the ratios between the baseline signal (prior to injection) and the signals at different time points following the injection were calculated. All the analysis was carried out using MATLAB.

3. RESULTS

3.1 Whole-body imaging

fSVOT employs continuous overfly scanning of the spherical array probe between head and tail of the mice in a zig-zag trajectory as shown in Fig. 1. For each laser pulse excitation, the system captures $\approx 1~\rm cm^3$ individual volumetric frames. A sequence of OA volumetric frames was acquired from a mouse at a scanning velocity of 80 mm/s velocity and 1064 nm excitation wavelength. This yielded a separation of 0.8 mm between consecutive frames over a single vertical sweep of the spherical array probe. Owing to the large FOV of the array detector, consecutive frames are overlapped and share anatomical information. By adding up consecutive frames over a single vertical sweep, a large FOV can be covered from head to tail of the mice within 1 s duration. Following full translation and rotation cycles, individual volumetric images are combined to form a whole-body image. In this way, 3D total-body scan with $\approx 200~\mu m$ spatial resolution is accomplished within 45 s at 80 mm/s scan velocity without relying on signal averaging. The maximum intensity projections (MIPs) of whole-body of mouse is shown in Fig. 2. A detailed anatomical information of the thorax and abdominal regions can be easily discerned with high resolution and contrast, showcasing various major organs such as heart, liver, spleen, kidneys, as well as spinal cord and the surrounding vasculature. Finer structures such as thoracic and femoral vessels can also be distinguished.

3.2 In vivo biodistribution of gold nanoparticles

In the cancer research field, gold nanoparticles (AuNPs) have shown to offer promising theranostic properties $^{16, 17}$, yet safety concerns related to accumulation and elimination from the body call for a better understanding of their pharmacokinetics and biocompatibility. Accumulation level and kinetics of excretion in the selected organs is directly linked to the potential toxicity of the injected agents. Here, we exploited the high spatiotemporal resolution performance of the fSVOT for visualizing the fast kinetics and biodistribution of AuNPs having peak absorption at 1070 nm wavelength. Generally, the clearance mechanism of substances from the blood circulation occurs either by being filtered in the kidneys or metabolized in the liver. Also, some of them are known to accumulate in the spleen. Generally, the two main sites of accumulation of AuNPs is in spleen and liver *in vivo*. Using fSVOT we were able to scan whole-body in 360° between thorax and abdominal regions at 80 mm/s within ≈ 45 s scan time. This allowed for longitudinal tracking of AuNPs kinetics simultaneously in multiple anatomical locations.

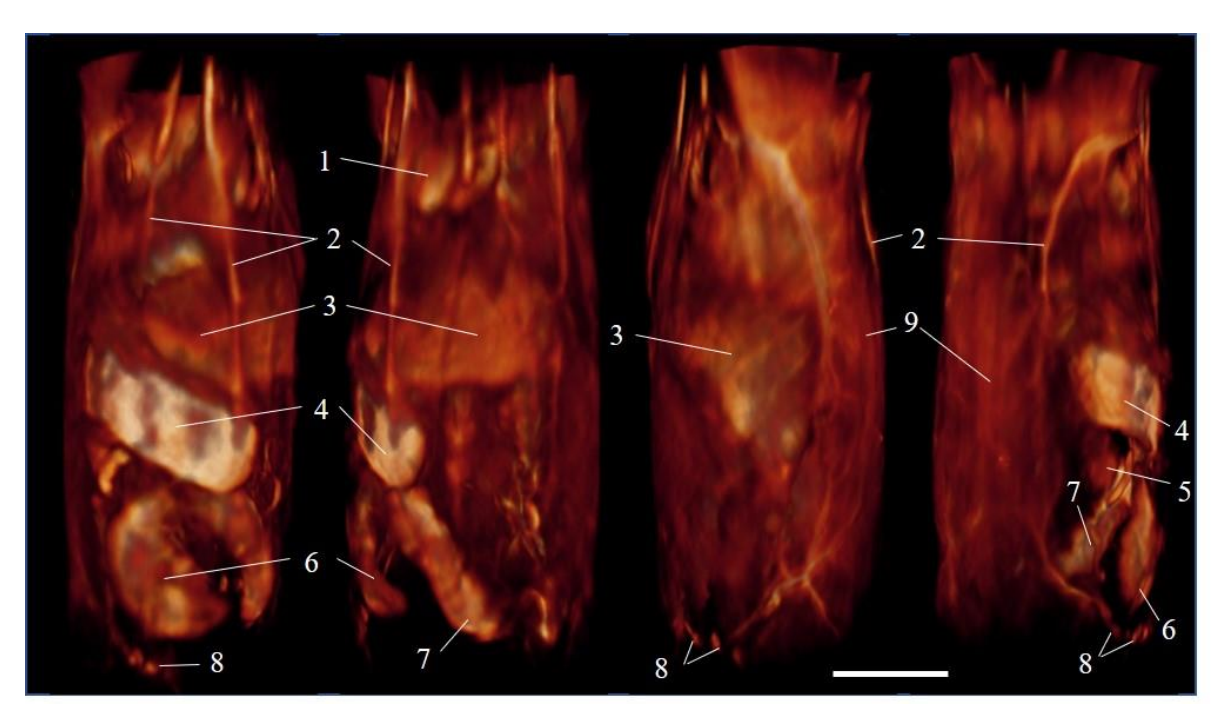


Figure 2. Whole-body 3D maximum intensity projection (MIP) images acquired within 45 s scan time at 80 mm/s scanning velocity. 1. Heart, 2. Thoracic vessels, 3. Liver, 4. Spleen, 5. Kidney, 6. Cecum, 7. Duodenum, 8. Femoral vessels, 9. Spine. Scale bar: 1cm.

The accumulation of AuNPs in spleen and liver are shown in Fig. 3a, and 3b respectively. Generally, there will be signal increase throughout the whole-body of mice as the agent circulates initially in entire vascular anatomy. This corresponds to signal increment in the kidneys (Fig. 3c) post 1 min injection and then gradually decreases corresponding to the agent accumulation in liver and spleen. We have quantified the percentage signal change in amplitude in spleen, liver, and kidneys (n = 3 mice) with respect to the base signal (before injection) as shown in Fig. 3d. Initially, the spleen accumulation increased to $\approx 30\%$ above the baseline post 1 min injection and then reached plateau gradually. On the other hand, the liver accumulation levelled off at 44% above the base line at 3 min after AuNP administration. A negative signal (signal decrease) might have been caused by a number of measurement imperfections not directly related to the probe concentration, such as slight motion of the mouse during the injections, laser energy instabilities, and light intensity variations inside the mouse due to an increased tissue absorption by the contrast agent.

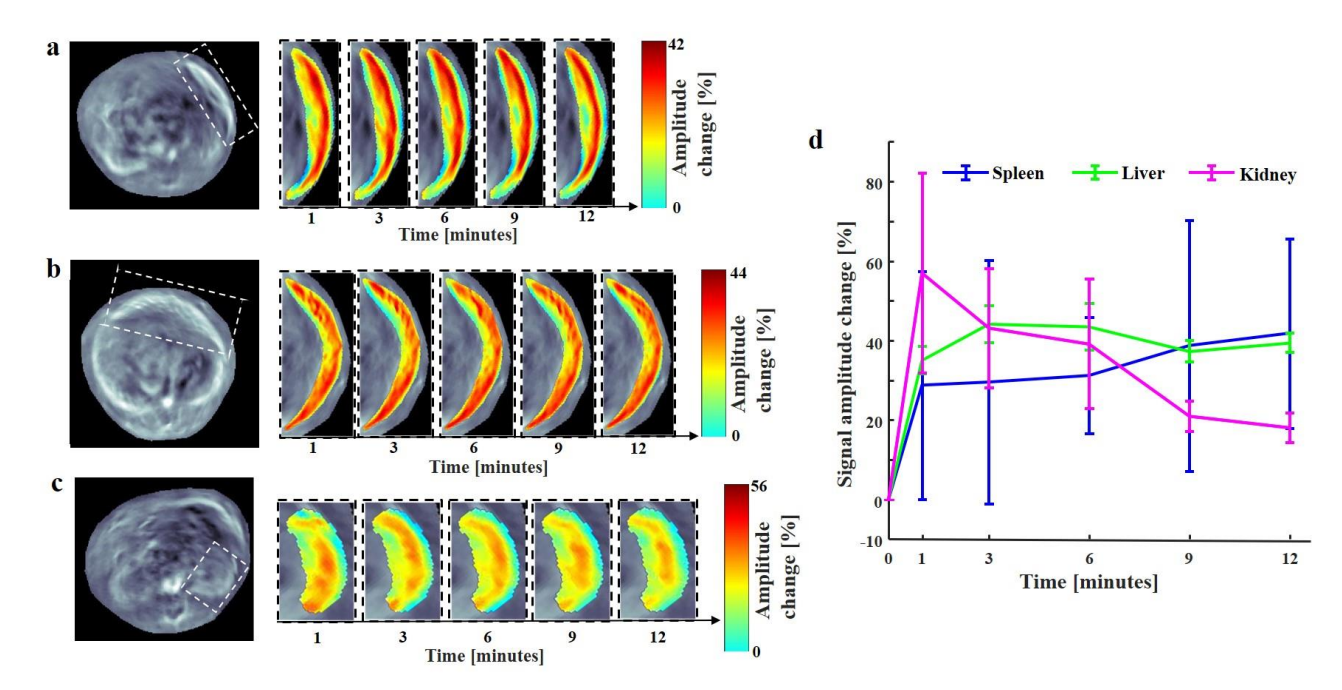


Figure 3. Whole-body tracking of kinetics using fSVOT. a) Cross-sectional images showing OA signal increase due to AuNP accumulation in the spleen. The zoom-ins display the OA signal amplitude changes in a single slice over time (superimposed in color) in response to AuNP administration. b) The corresponding slice images showing AuNP accumulation in the liver. c) The corresponding slice images showing no agent perfusion in the kidneys. d) Volumetric OA signal changes (baseline subtracted) measured across the whole liver, spleen, and kidney regions, following injection of AuNP (n = 3 mice).

4. DISCUSSIONS AND CONCLUSION

We present high spatiotemporal resolution based fSVOT technique for rapid anatomical and functional imaging of small animals. By employing continuous overfly scanning of the spherical array probe assisted with high micrometer-scale precision readings from laser distance sensor, whole body imaging of mice with full 360° coverage was achieved in 45 s scan time at 200 μ m resolution. This corresponds to more than an order of magnitude acceleration of the whole-body image acquisition speed compared to previously reported state-of-the-art SVOT system¹². This step change in performance has aided imaging of fast kinetics and biodistribution of optical contrast agents not possible with the previously reported approaches. The high speed imaging of fSVOT is comparable to state-of-the-art anatomical micro-CT scanners¹⁸ and greatly outperforms scan times of MRI or PET¹⁹.

Dynamic monitoring of agents in 3D on a whole-body scale by simultaneously tracking the pharmacokinetics of the AuNPs across several major organs such as spleen, liver, and kidneys has been showcased. In previously reported works, OA tracking of nanoagents in mice has been accomplished with typical total-body scanning times of several hours²⁰, or, alternatively, by confining detection to a single cross-section^{21, 22}. Taking advantage of fast scanning times that can be achieved using fSVOT, settling times of different organs could readily be discerned. At present, only micro-CT was shown to render similar throughput. However, it provides significantly lower sensitivity to AuNP and other extrinsic agents²³ and the use of harmful ionizing radiation is a great downside. The fSVOT imaging system further offers a broad selection of contrast molecules and nanoparticles not detectable with other well-established modalities such as PET or MRI. This is because any substance with distinct optical absorption characteristics may serve for optoacoustic contrast enhancement.

In summary, we demonstrated the feasibility of rapid volumetric OA tracking of nanoparticle kinetics in whole body of mice. The continuous scanning approach employed in fSVOT boosts the throughput capacity of OAT while enabling time-lapse multiplexed observations into early agent accumulation across multiple organs. Whole-body imaging on sub-minute time scales with rich contrast and resolution offers new venues for studying pharmacokinetics and pharmacodynamics of nanoparticulate agents, their accumulation, and clearance mechanisms in health and disease. Over

all, fSVOT can be employed for preclinical whole-body anatomical, functional and molecular imaging of pharmacokinetics and biodistribution with unprecedented high contrast, resolution, and speed.

ACKNOWLEDGEMENT

The authors would like to acknowledge the European Research Council under grant ERC-2015-CoG-682379.

REFERENCES

- 1. M. Baker, "The whole picture," *Nature* **463**(7283), 977-979 (2010).
- 2. R. Weissleder, and M. Nahrendorf, "Advancing biomedical imaging," *Proceedings of the National Academy of Sciences* **112**(47), 14424-14428 (2015).
- 3. K. O. Vasquez, C. Casavant, and J. D. Peterson, "Quantitative whole body biodistribution of fluorescent-labeled agents by non-invasive tomographic imaging," *PloS one* **6**(6), e20594 (2011).
- 4. J. R. Conway, N. O. Carragher, and P. Timpson, "Developments in preclinical cancer imaging: innovating the discovery of therapeutics," *Nat Rev Cancer* **14**(5), 314-328 (2014).
- 5. G. C. Kagadis et al., *Handbook of small animal imaging: preclinical imaging, therapy, and applications*, CRC Press (2016).
- 6. X. Deán-Ben et al., "Advanced optoacoustic methods for multiscale imaging of in vivo dynamics," *Chemical Society reviews* **46**(8), 2158-2198 (2017).
- 7. J. Weber, P. C. Beard, and S. E. Bohndiek, "Contrast agents for molecular photoacoustic imaging," *Nature Methods* **13**(8), 639-650 (2016).
- 8. K. Basak et al., "Non-invasive determination of murine placental and foetal functional parameters with multispectral optoacoustic tomography," *Light Sci Appl* **8**(71 (2019).
- 9. L. Li et al., "Single-impulse Panoramic Photoacoustic Computed Tomography of Small-animal Whole-body Dynamics at High Spatiotemporal Resolution," *Nature Biomedical Engineering* **1**(5), 0071 (2017).
- 10. S. Ermilov et al., "Three-dimensional optoacoustic and laser-induced ultrasound tomography system for preclinical research in mice: design and phantom validation," *Ultrasonic imaging* **38**(1), 77-95 (2016).
- 11. T. F. Fehm et al., "In vivo whole-body optoacoustic scanner with real-time volumetric imaging capacity," *Optica* **3**(11), 1153-1159 (2016).
- 12. X. L. Deán-Ben et al., "Spiral volumetric optoacoustic tomography visualizes multi-scale dynamics in mice," *Light: Science & Applications* **6**(4), e16247 (2017).
- 13. A. Ron et al., "Flash scanning optoacoustic tomography for high resolution whole-body tracking of nanoagent kinetics and biodistribution," *Laser & Photonics Reviews* (DOI:10.1002/lpor.202000484) (2021).
- 14. X. L. Dean-Ben, and D. Razansky, "Portable spherical array probe for volumetric real-time optoacoustic imaging at centimeter-scale depths," *Optics Express* **21**(23), 28062-28071 (2013).
- 15. X. L. Dean-Ben, A. Ozbek, and D. Razansky, "Volumetric real-time tracking of peripheral human vasculature with GPU-accelerated three-dimensional optoacoustic tomography," *IEEE Transations in Medical Imaging* **32**(11), 2050-2055 (2013).

- 16. A. R. Rastinehad et al., "Gold nanoshell-localized photothermal ablation of prostate tumors in a clinical pilot device study," *Proceedings of the National Academy of Sciences* **116**(37), 18590-18596 (2019).
- 17. N. S. Abadeer, and C. J. Murphy, "Recent progress in cancer thermal therapy using gold nanoparticles," *The Journal of Physical Chemistry C* **120**(9), 4691-4716 (2016).
- 18. S. J. Schambach et al., "Vascular imaging in small rodents using micro-CT," *Methods* **50**(1), 26-35 (2010).
- 19. F. Kiessling, B. Pichler, and P. Hauff, "How to Choose the Right Imaging Modality," in *Small Animal Imaging*, pp. 155-161, Springer (2017).
- 20. R. Su et al., "Three-dimensional optoacoustic imaging as a new noninvasive technique to study long-term biodistribution of optical contrast agents in small animal models," *Journal of biomedical optics* **17**(10), 101506 (2012).
- 21. J. Wang et al., "In vivo pharmacokinetic features and biodistribution of star and rod shaped gold nanoparticles by multispectral optoacoustic tomography," *RSC advances* **5**(10), 7529-7538 (2015).
- 22. S. P. Egusquiaguirre et al., "Optoacoustic imaging enabled biodistribution study of cationic polymeric biodegradable nanoparticles," *Contrast media & molecular imaging* **10**(6), 421-427 (2015).
- 23. R. Cheheltani et al., "Tunable, biodegradable gold nanoparticles as contrast agents for computed tomography and photoacoustic imaging," *Biomaterials* **102**(87-97 (2016).